Singular cases of planar and spatial C^1 Hermite interpolation problems based on quintic Pythagorean-hodograph curves

Rida T. Farouki · Kai Hormann · Federico Nudo

Abstract

A well-known feature of the Pythagorean-hodograph (PH) curves is the multiplicity of solutions arising from their construction through the interpolation of Hermite data. In general, there are four distinct planar quintic PH curves that match first-order Hermite data, and a two-parameter family of spatial quintic PH curves compatible with such data. Under certain special circumstances, however, the number of distinct solutions is reduced. The present study characterizes these singular cases, and analyses the properties of the resulting quintic PH curves. Specifically, in the planar case it is shown that there may be only three (but not less) distinct Hermite interpolants, of which one is a "double" solution. In the spatial case, a constant difference between the two free parameters reduces the dimension of the solution set from two to one, resulting in a family of quintic PH space curves of different shape but identical arc lengths. The values of the free parameters that result in formal specialization of the (quaternion) spatial problem to the (complex) planar problem are also identified, demonstrating that the planar PH quintics, including their degenerate cases, are subsumed as a proper subset of the spatial PH quintics.

Citation Info

Journal
Computer Aided Geometric Design

Volume
82, October 2020

Article
101930, 13 pages

DOI
10.1016/j.cagd.2020.101930

1 Introduction

Pythagorean-hodograph (PH) curves are characterized by the fact that their hodograph (derivative) components satisfy a Pythagorean condition — that is, for a given function space, the sum of their squares coincides with the perfect square of a member of that space. The earliest and simplest instances [12] are the *polynomial* PH curves, and they have subsequently been generalized to rational PH curves [13, 18] and algebraic-trigonometric PH curves [19, 20]. The treatise [4] gives a comprehensive analysis of PH curves, and a survey of new developments since its appearance may be found in [9].

The distinctive nature of PH curves permits exact computation of various properties of interest in precision motion control, spatial kinematics, robotics, and related fields — such as arc lengths, offset (parallel) loci to planar curves, and rotation-minimizing frames defined on space curves. However, because of the non-linear nature of their formulations, PH curves are not compatible with the traditional control-point methodology[1] for construction and shape manipulation. Consequently, the use of first-order Hermite interpolants (that match prescribed end points and derivatives) has become the standard means of constructing planar and spatial polynomial PH curves. The simplest PH curves capable of solving the general first-order Hermite interpolation are the quintics, in the case of both planar [11] and spatial [6] data.

The construction of PH curves is greatly facilitated by the adoption of a suitable algebraic framework. For planar PH curves, this is based on complex variables [3], and in the spatial case the quaternion algebra may be invoked [2] to ensure rotation-invariance of the formulation. In both cases, a multiplicity of quintic PH curve solutions to the first-order Hermite interpolation arises. For planar data there are, in general, four distinct interpolants, and for spatial data there is typically a two-parameter family of interpolants. Consequently, it is necessary to develop methods to identify the "best" curve among these many solutions in both the planar and spatial cases [1, 6, 8, 11, 14, 17].

However it has not been previously recognized that, under certain special circumstances, the cardinality of the set of planar or spatial quintic PH curve interpolants to prescribed first-order Hermite data is reduced relative to the general case. The focus of the present study is to identify and characterize these degenerate cases, in order to establish a more comprehensive theory of Hermite interpolation by planar and spatial quintic PH curves.

The plan for the remainder of this paper is as follows. Section 2 offers a detailed analysis of the conditions under which the planar PH quintic Hermite interpolation problem admits fewer than four distinct solutions,

[1] The "rectifying control polygon" [15] provides a partial remedy to this problem.

in terms of both the pre-image polynomial coefficients and constraints on the curve end derivatives, and a number of special configurations of the end derivatives are characterized in full. Section 3 then considers spatial Hermite interpolants, based upon the quaternion representation, which incurs two free parameters. A fixed difference between these parameters is the main factor influencing the cardinality of the solution space. Moreover, specific values of the parameters yield a proper specialization to the planar Hermite interpolants including the degenerate cases. Finally, Section 4 summarizes the key results of this study.

2 Planar Hermite interpolants

In the complex-variable model [3], the Cartesian components of a plane curve are identified with the real and imaginary parts of a complex-valued function $\boldsymbol{r}(\xi) = x(\xi) + \mathrm{i}\, y(\xi)$ of a real parameter ξ. A planar PH curve $\boldsymbol{r}(\xi)$ may then be generated from a complex *pre-image polynomial* $\boldsymbol{w}(\xi) = u(\xi) + \mathrm{i}\, v(\xi)$ by integrating the expression $\boldsymbol{r}'(\xi) = \boldsymbol{w}(\xi)^2$, such that $x'(\xi) = u(\xi)^2 - v(\xi)^2$ and $y'(\xi) = 2u(\xi)v(\xi)$. The *parametric speed* of $\boldsymbol{r}(\xi)$ — that is, the derivative $\mathrm{d}s/\mathrm{d}\xi$ of arc length s with respect to the parameter ξ — is defined by the polynomial $\sigma(\xi) = |\boldsymbol{r}'(\xi)| = |\boldsymbol{w}(\xi)|^2 = u^2(\xi) + v^2(\xi)$. Consequently, the indefinite integral of $\sigma(\xi)$, namely the arc length function $s(\xi)$, is also a polynomial.

To construct a planar PH quintic $\boldsymbol{r}(\xi)$, $\xi \in [0,1]$ we employ a quadratic complex pre-image polynomial, specified in Bernstein form as

$$\boldsymbol{w}(\xi) = \boldsymbol{w}_0(1-\xi)^2 + \boldsymbol{w}_1 2(1-\xi)\xi + \boldsymbol{w}_2\xi^2, \tag{1}$$

and integrate $\boldsymbol{r}'(\xi) = \boldsymbol{w}(\xi)^2$. There are, in general, *four* distinct planar PH quintics that have specified end points $\boldsymbol{r}(0)$, $\boldsymbol{r}(1)$ and derivatives $\boldsymbol{r}'(0)$, $\boldsymbol{r}'(1)$. For simplicity we consider data specified in *canonical form*[2] as $\boldsymbol{r}(0) = \boldsymbol{p}_0 = 0$, $\boldsymbol{r}(1) = \boldsymbol{p}_1 = 1$, $\boldsymbol{r}'(0) = \boldsymbol{d}_0 = d_0 \exp(\mathrm{i}\,\theta_0)$, $\boldsymbol{r}'(1) = \boldsymbol{d}_1 = d_1 \exp(\mathrm{i}\,\theta_1)$ where $\theta_0, \theta_1 \in (-\pi, +\pi]$ and we assume that $d_0, d_1 > 0$.

2.1 Characterization of the pre-image polynomial

We consider here the conditions on the coefficients of (1) that correspond to fewer than four distinct interpolants, and in Section 2.2 we formulate them in terms of the derivatives $\boldsymbol{d}_0$, $\boldsymbol{d}_1$. To match these derivatives, we must have

$$\boldsymbol{w}_0^2 = \boldsymbol{d}_0 \qquad \text{and} \qquad \boldsymbol{w}_2^2 = \boldsymbol{d}_1, \tag{2}$$

and hence

$$\boldsymbol{w}_0 = s_0\sqrt{d_0}\exp\left(\mathrm{i}\,\tfrac{1}{2}\theta_0\right), \qquad \boldsymbol{w}_2 = s_1\sqrt{d_1}\exp\left(\mathrm{i}\,\tfrac{1}{2}\theta_1\right), \tag{3}$$

with $s_0 = \pm 1$ and $s_1 = \pm 1$. Also, interpolation of the end points implies that

$$\int_0^1 \boldsymbol{r}'(\xi)\,\mathrm{d}\xi = \frac{1}{5}\left(\boldsymbol{w}_0^2 + \boldsymbol{w}_0\boldsymbol{w}_1 + \frac{2\boldsymbol{w}_1^2 + \boldsymbol{w}_0\boldsymbol{w}_2}{3} + \boldsymbol{w}_1\boldsymbol{w}_2 + \boldsymbol{w}_2^2\right) = 1,$$

or equivalently

$$2\boldsymbol{w}_1^2 + 3(\boldsymbol{w}_0 + \boldsymbol{w}_2)\boldsymbol{w}_1 + 3\boldsymbol{w}_0^2 + 3\boldsymbol{w}_2^2 + \boldsymbol{w}_0\boldsymbol{w}_2 = 15. \tag{4}$$

Now since Equation (4) has (in general) two distinct solutions for $\boldsymbol{w}_1$, and the expressions (3) for $\boldsymbol{w}_0$ and $\boldsymbol{w}_2$ each incorporate a sign ambiguity, it might be thought that in general there are *eight* distinct interpolants to the prescribed Hermite data. However, if $(\boldsymbol{w}_0, \boldsymbol{w}_1, \boldsymbol{w}_2)$ is a solution of Equations (2) and (4), then $(-\boldsymbol{w}_0, -\boldsymbol{w}_1, -\boldsymbol{w}_2)$ is also a solution, that generates the same curve $\boldsymbol{r}(\xi)$. Hence, there are (in general) *four* distinct Hermite interpolants: all four may be generated by fixing either s_0 or s_1 and varying the other.

Proposition 1. *The planar PH quintic Hermite interpolation problem has only three distinct solutions if and only if $\boldsymbol{w}_0$ and $\boldsymbol{w}_2$ satisfy*

$$3(\boldsymbol{w}_0^2 + \boldsymbol{w}_2^2) - 2\boldsymbol{w}_0\boldsymbol{w}_2 - 24 = 0, \tag{5}$$

and it is not possible to have less than three distinct solutions.

[2] Any given Hermite data may be mapped to canonical form by subtracting $\boldsymbol{p}_0$ from $\boldsymbol{p}_0$ and $\boldsymbol{p}_1$, and then dividing $\boldsymbol{p}_1$, $\boldsymbol{d}_0$, $\boldsymbol{d}_1$ by $\boldsymbol{p}_1$.

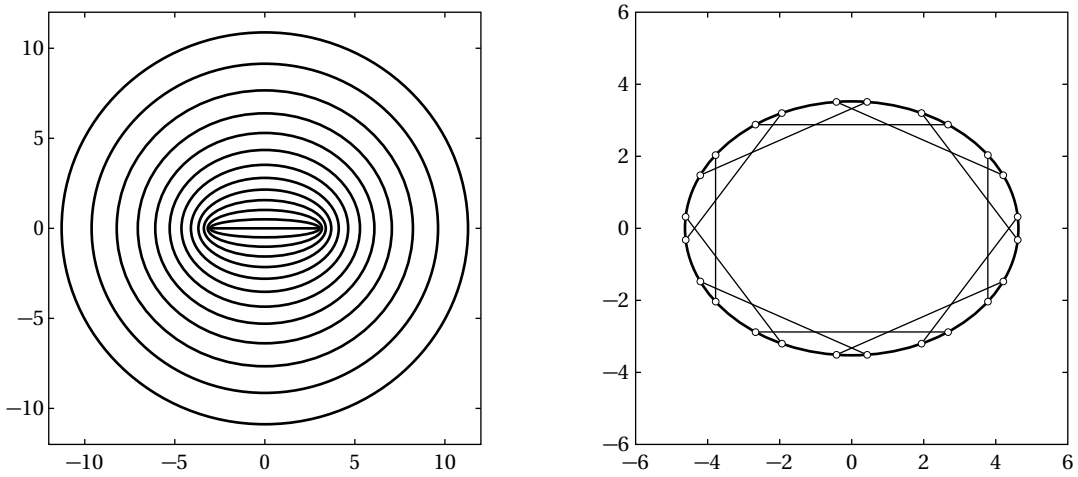

Figure 1: Left: the family of curves in the complex plane traced by $\boldsymbol{w}_0$, $\boldsymbol{w}_2$ over the domain $\alpha \in [0, 2\pi)$ for β varying between 0 and 2 in increments of 1/6. Right: correspondence of sampled values $\boldsymbol{w}_0$ and $\boldsymbol{w}_2$ satisfying (5) for $\beta = 1$.

Proof. When the discriminant of the quadratic equation (4) in $\boldsymbol{w}_1$ vanishes, it has a double root. On simplification, this yields the condition in (5). Equation (5) may be satisfied when s_0 and s_1 are either of like or unlike sign, but not both. If it is satisfied with $(s_0, s_1) = (1, 1)$ and $(-1, -1)$, these signs yield the same curve, but $(s_0, s_1) = (1, -1)$ and $(-1, 1)$ yield two distinct curves. Conversely, if it is satisfied with $(s_0, s_1) = (1, -1)$ and $(-1, 1)$, these signs yield the same curve, but $(1, 1)$ and $(-1, -1)$ yield two distinct curves. In both instances, we obtain three distinct interpolants (one of which may be considered a "double" solution). □

Remark 1. If Condition (5) is satisfied, Equation (4) has only one (double) root, namely $\boldsymbol{w}_1 = -\frac{3}{4}(\boldsymbol{w}_0 + \boldsymbol{w}_2)$.

With $\sin\psi = \sqrt{1/3}$ and $\cos\psi = \sqrt{2/3}$, the solutions to Equation (5) can be parameterized in terms of two real variables α and β as

$$\begin{aligned}\boldsymbol{w}_0 &= 3\sin(\alpha + \psi + \mathrm{i}\,\beta) = 3\big(\sin(\alpha+\psi)\cosh\beta + \mathrm{i}\cos(\alpha+\psi)\sinh\beta\big),\\ \boldsymbol{w}_2 &= 3\sin(\alpha - \psi + \mathrm{i}\,\beta) = 3\big(\sin(\alpha-\psi)\cosh\beta + \mathrm{i}\cos(\alpha-\psi)\sinh\beta\big).\end{aligned}$$

These expressions characterize $\boldsymbol{w}_0$ and $\boldsymbol{w}_2$ as lying on two families of curves, parameterized by the periodic variable $\alpha \in [0, 2\pi)$ and varying in shape with the non-periodic family parameter $\beta \in (-\infty, +\infty)$. The curves traced by $\boldsymbol{w}_0$ and $\boldsymbol{w}_2$ as α varies with β fixed are identical, since we can re-parameterize them by the new variables $\alpha_0 = \alpha + \psi$ and $\alpha_2 = \alpha - \psi$. However, the $\boldsymbol{w}_0$, $\boldsymbol{w}_2$ values that satisfy (5) are identified by *distinct* points on these curves.

Figure 1 shows examples, for $0 \le \beta \le 2$, of the loci traced by $\boldsymbol{w}_0$ and $\boldsymbol{w}_2$. These curves are ellipses with centres at the origin, and diameters $3\cosh\beta$ and $3\sinh\beta$ along the real and imaginary axes. The curves for negative and positive β values are mirror images of each other about the real axis, and they degenerate to the (doubly-traced) real interval $[-3, +3]$ when $\beta = 0$. Figure 1 also illustrates the correspondence of values $\boldsymbol{w}_0$ and $\boldsymbol{w}_2$ satisfying (5) in the case $\beta = 1$, identified by the angular displacement $\Delta\alpha = 2\psi \approx 70.5°$.

2.2 Constraints on end derivatives

On substituting from (3), the condition in (5) for only three distinct interpolants may be expressed in terms of the derivatives $\boldsymbol{d}_0$ and $\boldsymbol{d}_1$ as

$$3(\boldsymbol{d}_0 + \boldsymbol{d}_1) \pm 2\sqrt{\boldsymbol{d}_0\boldsymbol{d}_1} = 24, \tag{6}$$

or equivalently

$$3\big(d_0\exp(\mathrm{i}\,\theta_0) + d_1\exp(\mathrm{i}\,\theta_1)\big) \pm 2\sqrt{d_0 d_1}\exp\big(\mathrm{i}\,\tfrac{1}{2}(\theta_0+\theta_1)\big) = 24.$$

Setting $\theta_m = \frac{1}{2}(\theta_0 + \theta_1)$ and $\delta\theta = \frac{1}{2}(\theta_1 - \theta_0)$, so that $\theta_0 = \theta_m - \delta\theta$, $\theta_1 = \theta_m + \delta\theta$, upon conjugation and multiplication by $\exp(\mathrm{i}\,\theta_m)$ this becomes

$$3d_0\exp(\mathrm{i}\,\delta\theta) + 3d_1\exp(-\mathrm{i}\,\delta\theta) \pm 2\sqrt{d_0 d_1} = 24\exp(\mathrm{i}\,\theta_m). \tag{7}$$

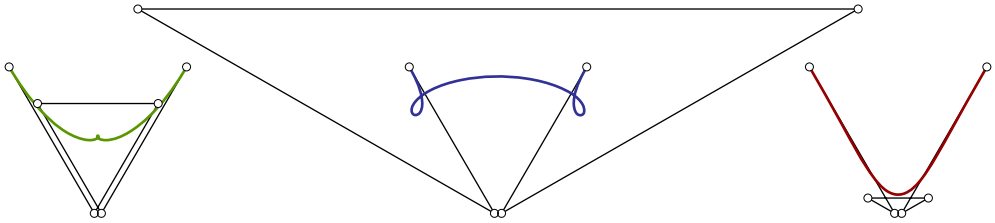

Figure 2: The three distinct PH quintic Hermite interpolants in Example 1 and their Bézier control polygons, including a "double" solution (green). The good interpolant free of tight loops (red) is one of the two "simple" solutions.

As previously noted, the condition in (7) may be satisfied with either the + sign or the − sign, but not both. The real and imaginary parts

$$3(d_0+d_1)\cos\delta\theta \pm 2\sqrt{d_0 d_1} = 24\cos\theta_m, \tag{8a}$$

$$3(d_0-d_1)\sin\delta\theta = 24\sin\theta_m, \tag{8b}$$

of Equation (7) define two real constraints on the four real values $d_0, d_1, \theta_0, \theta_1$.

2.2.1 Special cases

Before considering the general case, we consider three special circumstances: (i) derivatives of equal magnitude; (ii) derivatives of identical orientation; and (iii) one derivative is "flat" — that is, $\theta_0 = 0$ or $\theta_1 = 0$ (but not both). We begin with the analysis of case (i).

Proposition 2. *When $d_0 = d_1 = d$, there are only three distinct interpolants if and only if $\theta_0 = -\theta_1 = \theta$ with $\cos\theta > -1/3$ and $d = 12/(3\cos\theta \pm 1)$, where the value $d = 12/(3\cos\theta - 1)$ is valid only when $\cos\theta > 1/3$.*

Proof. When $d_0 = d_1 = d$, Condition (8b) is equivalent to $\sin\theta_m = 0$, that is, $\theta_m = 0$ or π. If $\theta_m = \pi$, then $\theta_0 = \theta_1 = \pi$ and $\delta\theta = 0$, so (8a) reduces to $6d \pm 2d = -24$, which has no valid positive solution for d. If $\theta_m = 0$ we have $\theta_0 = -\theta_1$, that is, $\boldsymbol{d}_0 = \overline{\boldsymbol{d}}_1$. Then with $\theta = \theta_0 = -\theta_1 = -\delta\theta$, Condition (8b) is automatically satisfied, and Condition (8a) becomes

$$3d\cos\theta \pm d = 12, \tag{9}$$

and hence $d = (3\cos\theta \pm 1)/12$. The restrictions on $\cos\theta$ follow from the requirement that $d > 0$. □

According to Proposition 2, two of the four PH quintic interpolants are coincident when the end derivatives are of equal magnitude, are symmetric about $\boldsymbol{r}(1)-\boldsymbol{r}(0)$, and the (unsigned) angle θ between them and $\boldsymbol{r}(1)-\boldsymbol{r}(0)$ is not too large. Specifically, if $\theta < \arccos(1/3) \approx 70.5°$ this occurs for two distinct derivative magnitudes d, whereas if $\arccos(1/3) \le \theta < \arccos(-1/3) \approx 109.5°$ it occurs for only one value of d. Conversely, it follows from (9) that for any common magnitude $d \ge 3$ of the end derivatives, there are only three distinct interpolants when $\theta = \arccos(4/d - 1/3)$. For $d \ge 6$, there is a second critical angle, $\theta = \arccos(4/d + 1/3)$, that admits only three distinct interpolants.

Example 1. For $\theta_m = 0$ and $\delta\theta = \arccos(1/2)$, the condition in (9) is satisfied with the plus sign — corresponding to unlike signs s_0, s_1 in (3) — by $d = 4.8$. With $\theta_0 = -\delta\theta$ and $\theta_1 = \delta\theta$, we then have

$$\boldsymbol{w}_0 = s_0 d\exp\left(-\mathrm{i}\tfrac{1}{2}\delta\theta\right), \qquad \boldsymbol{w}_2 = s_1 d\exp\left(\mathrm{i}\tfrac{1}{2}\delta\theta\right), \qquad \boldsymbol{w}_1 = -\tfrac{3}{4}(\boldsymbol{w}_0 + \boldsymbol{w}_2).$$

Since $\boldsymbol{w}(\xi)$ and $-\boldsymbol{w}(\xi)$ specify the same hodograph $\boldsymbol{r}'(\xi)$, the values $(s_0, s_1) = (-1, 1)$ and $(1, -1)$ generate the same curve. Two more distinct interpolants with equal end derivative magnitudes $d = 4.8$ exist, for which the condition in (5) is not satisfied, so Equation (4) has two distinct solutions $\boldsymbol{w}_1$. The curves generated by the standard PH quintic Hermite interpolation scheme are shown in Figure 2. Note that like signs s_0, s_1 yield $d = 24.0$ in (9), which specifies a different Hermite interpolation problem. Figure 3 shows further examples with $d_0 = d_1$ that admit only three distinct solutions.

Remark 2. As a special instance of the construction for end derivatives of equal magnitude, the case of interpolants to G^1 Hermite data with a specified arc length S has been addressed in [5]. It was shown that in general there are two distinct solutions (of which one has attractive shape properties and the other exhibits undesirable looping behaviour). Consistent with Proposition 2, these interpolants must satisfy $\sin\theta_m = 0$. Moreover, it was found that only *one* distinct solution exists when $\delta\theta$ satisfies $\cos\delta\theta = (S \pm 3)/(3S \pm 1)$.

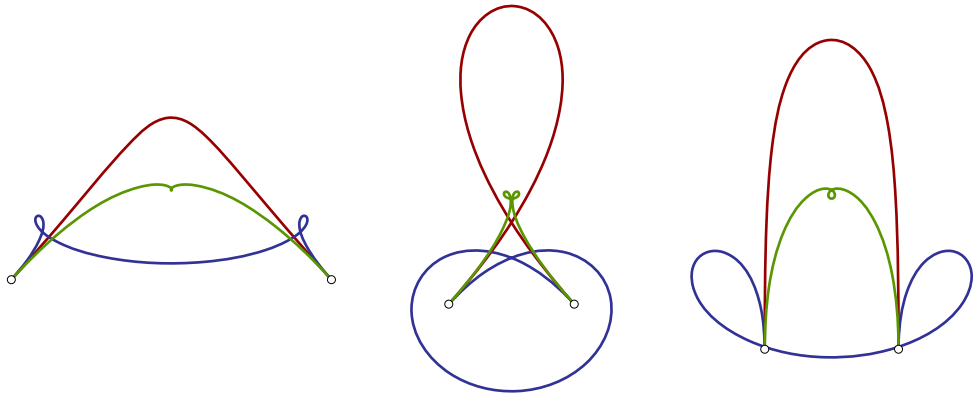

(a) (b) (c)

Figure 3: Examples of PH quintic Hermite interpolants for end derivatives of equal magnitude: (a) $d_0 = d_1 = 4$, $\theta_0 = -\theta_1 = \arccos(2/3)$; (b) $d_0 = d_1 = 12$, $\theta_0 = -\theta_1 = \arccos(2/3)$; (c) $d_0 = d_1 = 12$, $\theta_0 = -\theta_1 = \pi/2$. In all of these examples, the green curve corresponds to the "double" solution.

We now consider the case (ii): parallel end derivative orientations.

Proposition 3. *When $\theta_0 = \theta_1 = \theta$, there are only three distinct Hermite interpolants if and only if $\theta = 0$ and d_0, d_1 satisfy the condition*

$$9({d_0}^2 + {d_1}^2) + 14 d_0 d_1 - 144(d_0 + d_1) + 576 = 0. \tag{10}$$

This equation defines an ellipse in the (d_0, d_1) plane with centre at $(9/2, 9/2)$ and semi-axes 6 and $3/\sqrt{2}$, rotated by angle $-\pi/4$. The ellipse is tangent to its bounding box $[0,9] \times [0,9]$ at $(0,8), (8,0), (1,9), (9,1)$ — see Figure 4.

Proof. When $\theta_0 = \theta_1 = \theta$, we have $\theta_m = \theta$ and $\delta\theta = 0$, and (8b) simplifies to $\sin\theta = 0$, that is, $\theta = 0$ or π. If $\theta = 0$, then (8a) is equivalent to

$$3(d_0 + d_1) - 24 = \pm 2\sqrt{d_0 d_1}, \tag{11}$$

and we obtain (10) on squaring both sides. If $\theta = \pi$, Equation (8a) can be reduced to

$$9(d_0 - d_1)^2 + 32 d_0 d_1 + 144(d_0 + d_1) + 576 = 0,$$

which clearly has no solution with $d_0, d_1 > 0$ — in fact, this equation defines an ellipse similar to that defined by (10), but with centre $(-9/2, -9/2)$ and bounding box $[-9, 0] \times [-9, 0]$. □

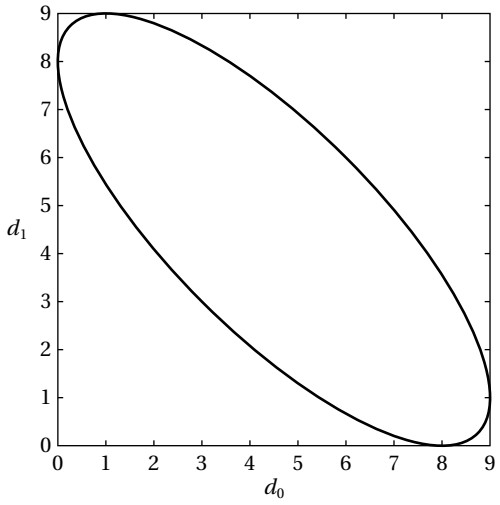

Figure 4: The set of derivative magnitudes (d_0, d_1) for which there are just three distinct PH quintic Hermite interpolants with $\theta_0 = \theta_1 = 0$.

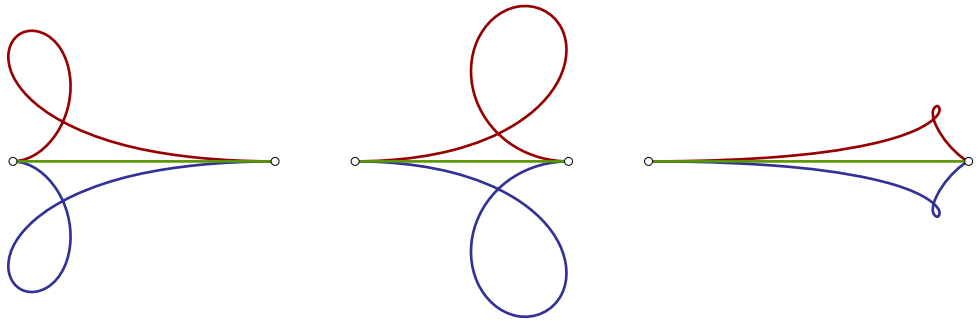

(a) (b) (c)

Figure 5: Examples of quintic PH Hermite interpolants for end derivatives with equal angles: (a) $\theta_0 = \theta_1 = 0$, $d_0 = 1$, $d_1 = 9$; (b) $\theta_0 = \theta_1 = 0$, $d_0 = 25/3$, $d_1 = 3$; (c) $\theta_0 = \theta_1 = 0$, $d_0 = 25/3$, $d_1 = 1/27$. In all examples, the green curve is the one corresponding to the "double" solution.

Figure 5 shows a few examples for the situation described in Proposition 3. It follows from the apparent symmetry of the interpolants about the line $\boldsymbol{r}(1)-\boldsymbol{r}(0)$, which is induced by the angles $\theta_0 = \theta_1 = 0$, that the "double" solution must trace out the line segment between $\boldsymbol{r}(0)$ and $\boldsymbol{r}(1)$.

Remark 3. The "upper arc" of the ellipse in Figure 4 from $(0,8)$ to $(8,0)$ corresponds to solutions (d_0, d_1) of (11) with the $+$ sign on the right, while the "lower arc" corresponds to solutions (d_0, d_1) with the $-$ sign on the right. The latter case occurs when the discriminant of Equation (4) vanishes with unlike signs s_0, s_1 in (3). Consequently, the discriminant of (4) with like signs s_0, s_1 is positive, so $\boldsymbol{w}_1$ is a real value as well as $\boldsymbol{w}_0, \boldsymbol{w}_2$ (since $\theta_0 = \theta_1 = 0$), for all three PH quintics. Hence, we obtain three distinct curves tracing the line segment $\boldsymbol{r}(0)$ to $\boldsymbol{r}(1)$ in this case. For (d_0, d_1) on the upper ellipse arc, the discriminant of (4) vanishes if s_0, s_1 are of like sign, giving the straight line $\boldsymbol{r}(0)$ to $\boldsymbol{r}(1)$ as a "double" curve; or it is negative if s_0, s_1 are of unlike signs, yielding two non-trivial but symmetric curves as shown in Figure 5.

We observe from Figure 4 and the previous remark that if $0 < d_0 \leq 8$ or $d_0 = 9$, there exists exactly one d_1 such that for $\theta_0 = \theta_1 = 0$ three distinct interpolants exist, but this is true for only two distinct d_1 values if $8 < d_0 < 9$. Moreover, for $0 < d_0 < 8$ a unique value of d_1 exists, such that there are three distinct solutions with the same shape, namely the straight line from $\boldsymbol{r}(0)$ to $\boldsymbol{r}(1)$. By symmetry, analogous results hold for d_0 when d_1 is given.

Finally, we treat case (iii): one derivative is "flat" but the other is not.

Proposition 4. *When $\theta_0 \neq 0 = \theta_1$, there are only three distinct interpolants if and only if $\cos\theta_0 > -7/9$ and $d_0 = 16/(7+9\cos\theta_0)$, $d_1 = d_0 + 8$.*

Proof. If $\theta_1 = 0$, then $\theta_m = -\delta\theta = \frac{1}{2}\theta_0$ and (8b) is equivalent to $d_1 = d_0 + 8$. Substituting this into (8a), we get

$$6d_0 \cos\theta_m = \pm 2\sqrt{d_0(d_0+8)},$$

and after squaring both sides and dividing by $4d_0$ we have

$$9d_0 \cos^2\theta_m = d_0 + 8. \tag{12}$$

Recalling that $\cos^2\theta_m = \frac{1}{2}(1+\cos\theta_0)$, this is equivalent to

$$d_0 = \frac{16}{7+9\cos\theta_0},$$

and d_0 is positive if and only if $\cos\theta_0 > -7/9$. □

By symmetry, Proposition 4 also holds if we swap the roles of θ_0, θ_1 and of d_0, d_1. Thus, if one end derivative points in the same direction as $\boldsymbol{r}(1)-\boldsymbol{r}(0)$ and the (unsigned) angle θ between the other end derivative and $\boldsymbol{r}(1)-\boldsymbol{r}(0)$ satisfies $\theta < \cos(-7/9) \approx 141.1°$, there exist unique magnitudes for each of the two end derivatives, such that there are only three distinct quintic PH Hermite interpolants, as shown in Figure 6.

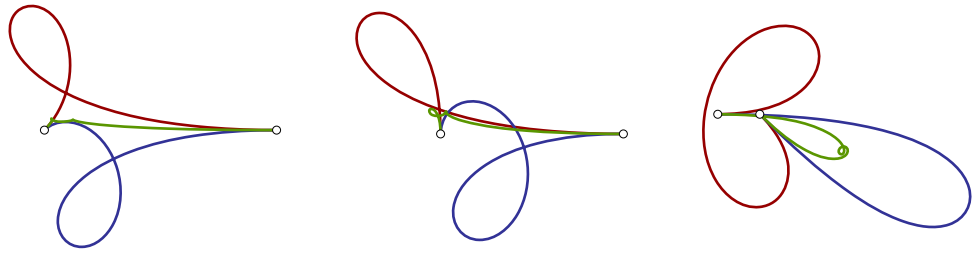

(a) (b) (c)

Figure 6: Examples of quintic PH Hermite interpolants for the case when one end derivative is flat but the other is not: (a) $\theta_0 = \pi/4$, $\theta_1 = 0$, $d_0 = 8(28-18\sqrt{2})/17$, $d_1 = 8(45-18\sqrt{2})/17$; (b) $\theta_0 = \pi/2$, $\theta_1 = 0$, $d_0 = 16/7$, $d_1 = 72/7$; (c) $\theta_0 = 0$, $\theta_1 = 3\pi/4$, $d_0 = 8(45+18\sqrt{2})/17$, $d_1 = 8(28+18\sqrt{2})/17$. In all cases, the green curve is the one corresponding to the "double" solution.

2.2.2 The general case

Setting $\delta d = \frac{1}{2}(d_1 - d_0)$ and $d_m = \frac{1}{2}(d_0 + d_1) > |\delta d|$, so that $d_0 = d_m - \delta d$ and $d_1 = d_m + \delta d$, we may write (8a) and (8b) as

$$3 d_m \cos\delta\theta - 12\cos\theta_m = \pm\sqrt{{d_m}^2 - \delta d^2}, \tag{13a}$$

$$\delta d \sin\delta\theta + 4\sin\theta_m = 0. \tag{13b}$$

As the case $\delta\theta = 0$ has already been treated in Proposition 3, we can assume without loss of generality that $\cos\delta\theta < 1$ and $\sin\delta\theta \neq 0$, since $\delta\theta \in (-\pi, \pi)$, and re-write (13b) as

$$\delta d = -\frac{4\sin\theta_m}{\sin\delta\theta}. \tag{14}$$

We further note that (13a), after squaring both sides, is equivalent to

$$(9\cos^2\delta\theta - 1){d_m}^2 + \delta d^2 - 72\cos\theta_m\cos\delta\theta\, d_m + 144\cos^2\theta_m = 0. \tag{15}$$

For any fixed θ_m and $\delta\theta$ (i.e., for any given θ_0 and θ_1) this quadratic equation in d_m and δd defines a conic section in the $(d_m, \delta d)$ plane: see Figures 7 and 8. Specifically, this conic section is

$$\left.\begin{array}{l}\text{an ellipse,}\\ \text{a parabola,}\\ \text{a hyperbola,}\end{array}\right\} \quad \text{when } \cos^2\delta\theta \left\{\begin{array}{l}>\\ =\\ <\end{array}\right\} \frac{1}{9}, \tag{16}$$

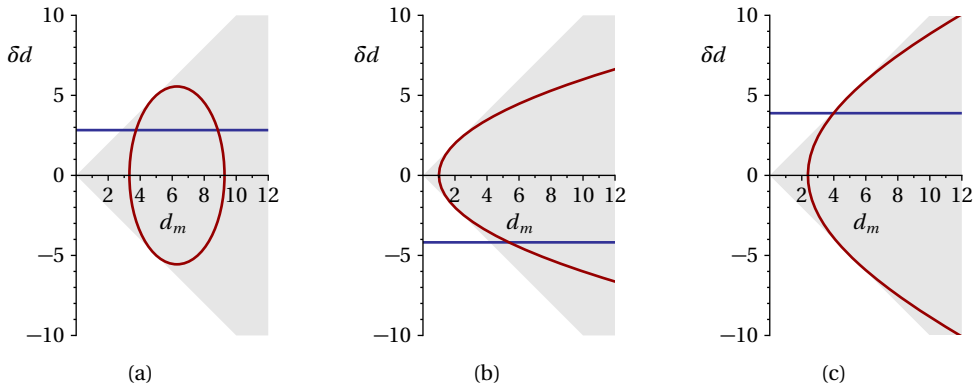

(a) (b) (c)

Figure 7: Examples of the line (blue) defined by (14) and the conic (red) given by (15): (a) $\theta_m = \pi/6$, $\delta\theta = -\pi/4$ (ellipse); (b) $\theta_m = \arccos(1/6)$, $\delta\theta = \arccos(1/3)$ (parabola); (c) $\theta_m = -3\pi/8$, $\delta\theta = 2\pi/5$ (hyperbola). The area $D_+ = \{(d_m, \delta d) : d_m > |\delta d|\}$ corresponding to valid magnitudes $d_0, d_1 > 0$ is shown in grey. Note that the conic sections touch the boundary of D_+.

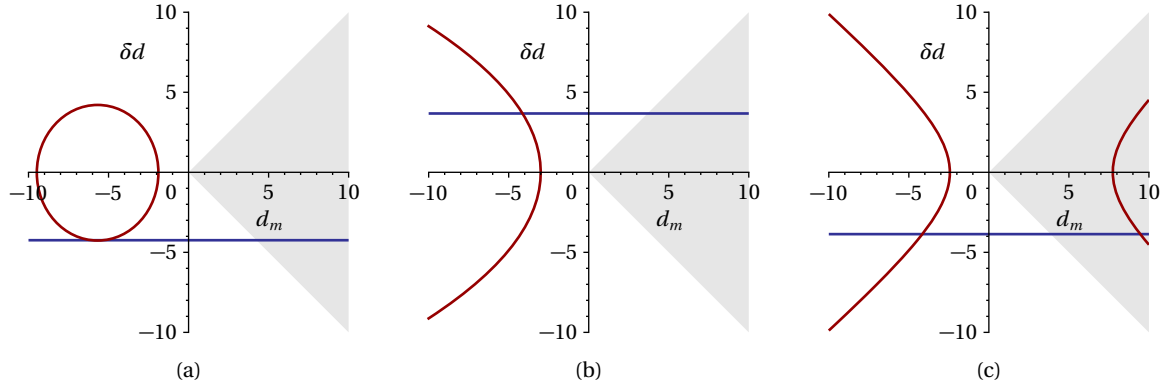

Figure 8: Further examples of the line (14) and the conic (15): (a) $\theta_m = \pi - \arctan(3\sqrt{15}/4)$, $\delta\theta = \pi/3$ (ellipse); (b) $\theta_m = 2\pi/3$, $\delta\theta = -\arccos(1/3)$ (parabola); (c) $\theta_m = 3\pi/5$, $\delta\theta = 4\pi/9$ (hyperbola).

and it is non-degenerate if and only if $|\theta_m| \neq \pi/2$. Consequently, there are only three distinct Hermite interpolants if and only if the line parallel to the d_m-axis defined by (14) intersects the conic section in (15), and there can be up to two intersections.

Before analysing these cases in detail, we make a few general observations regarding the quadratic polynomial $Q(d_m, \delta d)$ on the left hand side of (15). First, since it is an even function of δd, the conic section defined by its zero set is symmetric about the d_m-axis. Second, it is non-negative along the lines $\delta d = \pm d_m$ since it has the factorization

$$Q(d_m, \pm d_m) = 9(\cos\delta\theta\, d_m - 4\cos\theta_m)^2, \tag{17}$$

and it vanishes along these lines, if and only if either (i) $\cos\delta\theta = \cos\theta_m = 0$ (which implies that $\theta_0 = 0$ or $\theta_1 = 0$, and this case has been discussed in Proposition 4), or $\cos\delta\theta \neq 0$ and

$$d_m = \frac{4\cos\theta_m}{\cos\delta\theta} =: d^*. \tag{18}$$

In the latter case, the conic section is tangent to the lines $\delta d = \pm d_m$ at the points $(d_m, \delta d) = (d^*, \pm d^*)$, because the gradient at these points where Q vanishes simplifies to

$$\nabla Q(d^*, \pm d^*) = 2d^*(-1, \pm 1). \tag{19}$$

We begin by investigating the case of the ellipse in (16).

Proposition 5. *When $1/9 < \cos^2\delta\theta < 1$, the Hermite interpolation problem has three distinct solutions if and only if we have $\cos\theta_m \cos\delta\theta > 0$,*

$$|\tan\theta_m| \leq \frac{3|\sin\delta\theta|}{\sqrt{9\cos^2\delta\theta - 1}}, \tag{20}$$

δd is given by (14), and d_m is either solution of the quadratic equation (15), which has just one solution if (20) holds with equality. Moreover, if $|\theta_m| = |\delta\theta|$, the smaller value of d_m does not identify a valid configuration.

Proof. If $\cos^2\delta\theta > 1/9$, the centre of the ellipse defined by (15) lies on the positive d_m-axis if and only if $\cos\theta_m \cos\delta\theta > 0$, which implies that d^* in (18) is positive. By (17) and (19), the ellipse is contained within the open sector $D_+ = \{(d_m, \delta d) : d_m > |\delta d|\}$ in this case, except for the two points $(d^*, \pm d^*)$ that lie on the boundary ∂D_+ of D_+. Since the length of the δd-semi-axis is

$$\frac{12|\cos\theta_m|}{\sqrt{9\cos^2\delta\theta - 1}},$$

the line (14) intersects the ellipse if and only if condition (20) holds, with only one intersection in the case of equality.

It remains to exclude the instance in which the line intersects the ellipse at $(d^*, \pm d^*)$, as this corresponds to an invalid configuration with $d_0 = 0$ or $d_1 = 0$. This happens if and only if δd in (14) is equal to d^* or $-d^*$, that is,

$$\frac{\sin\theta_m}{\sin\delta\theta} = \pm\frac{\cos\theta_m}{\cos\delta\theta},$$

which in turn is equivalent to $\sin(\theta_m \pm \delta\theta) = 0$. Since $\theta_m \pm \delta\theta = \pm\pi$ implies $\cos\theta_m \cos\delta\theta \leq 0$, we conclude that this special case occurs if $\theta_m \pm \delta\theta = 0$, or equivalently if $|\theta_m| = |\delta\theta|$. □

Note that the case $|\theta_m| = \pi/2$, which leads to a degenerate ellipse — that is, the single point at $(0,0)$ — and hence does not identify a valid configuration, is ruled out by Condition (20). Furthermore, in the special case $\theta_m = -\delta\theta$ (for which $\theta_1 = 0$ and $\delta d = d^*$), we have $d_m = d^* = 4$, and the second valid configuration of magnitudes d_0, d_1 is the one given in Proposition 4, and likewise for the case $\theta_m = \delta\theta$ (for which $\theta_0 = 0$ and $\delta d = d^*$). The invalid configuration $d_0 = 0$, $d_1 = 8$ is ruled out in the proof of Proposition 4 when we divide by $d_0 > 0$ to arrive at (12).

We now turn our attention to the case of the parabola in (16).

Proposition 6. *When* $\cos^2\delta\theta = 1/9$, *the Hermite interpolation problem has three distinct solutions if and only if* $\cos\theta_m \cos\delta\theta > 0$, $|\theta_m| \neq |\delta\theta|$, δd *is given by* (14), *and*

$$d_m = \left(\frac{3}{4}\tan^2\theta_m + 6\right)|\cos\theta_m|. \tag{21}$$

Proof. When $\cos^2\delta\theta = 1/9$, the parabola in (15) lies in the open half-plane $H = \{(d_m, \delta d) : d_m > 0\}$ if and only if $\cos\theta_m \cos\delta\theta > 0$. As in the proof of Proposition 5, this implies that d^* in (18) is positive and that the parabola is contained in D_+, except for the two points $(d^*, \pm d^*) \in \partial D_+$. In this case, since the parabola is symmetric about the d_m-axis, there is exactly one intersection of the line (14) with it. Noting that

$$\delta d^2 = \frac{16\sin^2\theta_m}{\sin^2\delta\theta} = \frac{16\sin^2\theta_m}{1-\cos^2\delta\theta} = 18\sin^2\theta_m,$$

it follows from (15) that the d_m coordinate of this intersection point is

$$d_m = \frac{\delta d^2 + 144\cos^2\theta_m}{72\cos\theta_m\cos\delta\theta} = \frac{18\sin^2\theta_m + 144\cos^2\theta_m}{24|\cos\theta_m|},$$

which simplifies to (21). As in the proof of Proposition 5, it follows that the special case of an intersection on the boundary of D_+, which does not give a valid configuration, happens if and only if $|\theta_m| = |\delta\theta|$. □

It remains to analyse the case of the hyperbola in (16).

Proposition 7. *When* $\cos^2\delta\theta < 1/9$, *the Hermite interpolation problem has three distinct solutions if and only if either* $\cos\theta_m\cos\delta\theta < 0$ *or* $|\theta_m| \neq |\delta\theta|$, δd *is given by* (14), *and* d_m *is the larger of the two solutions of the quadratic equation* (15), *which is guaranteed to be greater than* $|\delta d|$.

Proof. If $\cos^2\delta\theta < 1/9$, the centre of the hyperbola defined by (15) is located on the d_m-axis at the point

$$\left(\frac{36\cos\theta_m\cos\delta\theta}{9\cos^2\delta\theta - 1}, 0\right).$$

If $\cos\theta_m\cos\delta\theta < 0$, then d^* in (18) is negative and, by (17) and (19), one branch of the hyperbola touches the boundary of the open sector $D_- = \{(d_m, \delta d) : -d_m > |\delta d|\}$. As the centre of the hyperbola lies on the positive d_m-axis in this case, the other branch of the hyperbola is contained in D_+ and has a unique intersection with the line in (14), corresponding to valid magnitudes $d_0, d_1 > 0$.

If $\cos\theta_m\cos\delta\theta > 0$, then d^* in (18) is positive, one branch of the hyperbola touches D_+ at the two points $(d^*, \pm d^*) \in \partial D_+$, and the other lies in D_-. Thus, there is a unique intersection of the line (14) and the hyperbola in D_+, except if $|\theta_m| = |\delta\theta|$, when this intersection occurs at the touching points.

The previous line of argument extends to the case $\cos\delta\theta = 0$, $\cos\theta_m \neq 0$, when the hyperbola is a rectangular hyperbola with centre at $(0,0)$ and to the case $\cos\delta\theta \neq 0$, $\cos\theta_m = 0$, when the hyperbola degenerates into a pair of lines intersecting at $(0,0)$. In the remaining case $\cos\delta\theta = \cos\theta_m = 0$, which is equivalent to $|\theta_m| = |\delta\theta| = \pi/2$, the line in (14) intersects the degenerate rectangular hyperbola on the boundary of D_+ at $(4,4)$ or $(4,-4)$. □

If $\delta\theta = -\pi/2$, which implies that $\cos\delta\theta = 0$ so $\boldsymbol{d}_0$ and $\boldsymbol{d}_1$ point in opposite directions, we can further deduce that the PH quintic Hermite interpolation problem has only three distinct solutions if and only if

$$d_0 = 4\sqrt{1+8\cos^2\theta_m} + 4\sin\theta_m, \qquad d_1 = 4\sqrt{1+8\cos^2\theta_m} - 4\sin\theta_m.$$

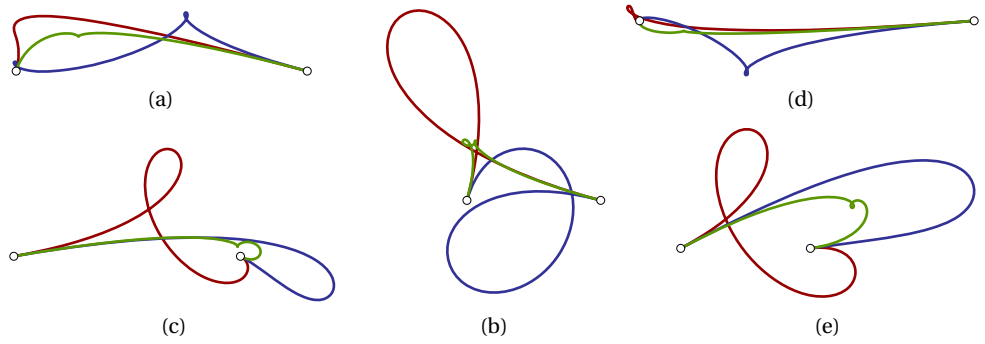

Figure 9: Example quintic PH curves for the cases in Figures 7 and 8: (a) ellipse, first intersection; (b) ellipse, second intersection; (c) parabola; (d) hyperbola in Figure 7; (e) hyperbola in Figure 8. The θ_0, θ_1 and d_0, d_1 values for these examples are listed in Table 1. In each case, the green curve corresponds to the "double" solution.

	θ_0	θ_1	d_0	d_1
(a)	$5\pi/12$	$-\pi/12$	$2(9\sqrt{6}-4\sqrt{5}-7\sqrt{2})/7$	$2(9\sqrt{6}-4\sqrt{5}+7\sqrt{2})/7$
(b)	$5\pi/12$	$-\pi/12$	$2(9\sqrt{6}+4\sqrt{5}-7\sqrt{2})/7$	$2(9\sqrt{6}+4\sqrt{5}+7\sqrt{2})/7$
(c)	~ 0.1724	~ 2.634	$43/8+\sqrt{70}/2,$	$43/8-\sqrt{70}/2$
(d)	$-31\pi/40$	$\pi/40$	~ 0.1018	~ 7.873
(e)	$7\pi/45$	$47\pi/45$	~ 13.32	~ 5.599

Table 1: Values of θ_0, θ_1 and d_0, d_1 for the examples in Figure 9.

For $\theta_m = 0$ this reduces to $d_0 = d_1 = 12$, and we obtain the example in Figure 3 (c). As $\theta_m \to \pm\pi/2$ and $\boldsymbol{d}_0, \boldsymbol{d}_1$ become parallel to $\boldsymbol{r}(1)-\boldsymbol{r}(0)$, one of d_0, d_1 approaches 0, an invalid configuration. Similar results hold for $\delta\theta = \pi/2$.

If $\theta_m = \pi/2$, so that $\cos\theta_m = 0$ and $\boldsymbol{d}_0, \boldsymbol{d}_1$ are symmetric about the normal to the line from $\boldsymbol{r}(0)$ to $\boldsymbol{r}(1)$, then if they are sufficiently close to this line — since we require $\cos^2\delta\theta = \sin^2\theta_0 = \sin^2\theta_1 < 1/9$ — the critical end derivative magnitudes for just three PH quintic Hermite interpolants are

$$d_0 = \frac{4}{|\sin\delta\theta|\sqrt{1-9\cos^2\delta\theta}} + \frac{4}{\sin\delta\theta}, \qquad d_1 = \frac{4}{|\sin\delta\theta|\sqrt{1-9\cos^2\delta\theta}} - \frac{4}{\sin\delta\theta}.$$

Consistent with previous observations, one of these magnitudes converges to 0 as $\delta\theta \to \pm\pi/2$. Similar conclusions hold for the case $\theta_m = -\pi/2$. Examples illustrating these different cases are shown in Figure 9.

Figure 10 summarizes the above results graphically in the (θ_0, θ_1) domain. The red regions correspond to the ellipse case (Proposition 5), with the curved boundaries marking the situation when the line (14) is tangent to the ellipse. The hyperbola case (Proposition 7) is indicated in blue, and the boundary between red and blue regions represents the parabola case in Proposition 6. The coloured dashed lines ($\theta_0 = 0$ and $\theta_1 = 0$) indicate the special case $|\theta_m| = |\delta\theta|$, when one of the magnitudes that lead to the loss of a PH quintic interpolant is zero and hence to an invalid configuration, and the solutions along the blue part of these dashed lines are given by Proposition 4. The behaviour along the black dashed line ($\theta_m = 0$) is described in Proposition 2, and Proposition 3 captures the situation along the dotted black line ($\delta\theta = 0$), including the purple origin of the plot, which indicates the multitude of possible lengths that yield a degenerate interpolation problem (see Figure 4).

3 Spatial Hermite interpolants

To ensure *rotation invariance* of spatial PH curves (i.e., an algebraic structure independent of the coordinate axes [7]), we use the quaternion representation [2]. Recall that a quaternion $\mathcal{Q} = (q, \boldsymbol{q})$ comprises a scalar part q and a vector part $\boldsymbol{q}$. The pure scalar and pure vector quaternions $(q, 0)$ and $(0, \boldsymbol{q})$ may be written as q and $\boldsymbol{q}$, and the norm and conjugate of $\mathcal{Q}$ are $|\mathcal{Q}| = \sqrt{q^2 + |\boldsymbol{q}|^2}$ and $\mathcal{Q}^* = (q, -\boldsymbol{q})$. The sum of two quaternions $\mathcal{A} = (a, \boldsymbol{a})$ and $\mathcal{B} = (b, \boldsymbol{b})$ is $\mathcal{A} + \mathcal{B} = (a + b, \boldsymbol{a} + \boldsymbol{b})$, and the product can be expressed as

$$\mathcal{A}\mathcal{B} = (a\,b - \boldsymbol{a}\cdot\boldsymbol{b}, a\boldsymbol{b} + b\,\boldsymbol{a} + \boldsymbol{a}\times\boldsymbol{b}).$$

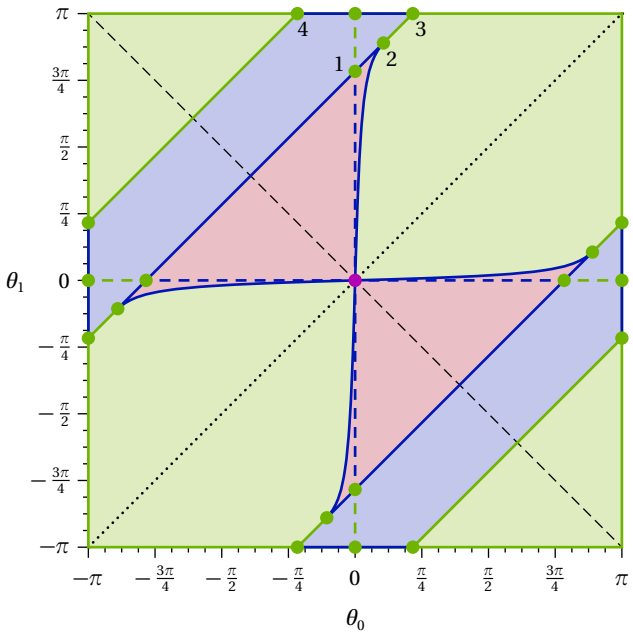

Figure 10: Graph of the dependence on (θ_0,θ_1) of the number of derivative magnitude pairs (d_0,d_1) that admit just three distinct PH quintic Hermite interpolants. There may be just one pair (blue), two pairs (red), or multiple pairs (purple). For most angles (green), there are four distinct interpolants for all positive (d_0,d_1) values. The numbered green points have coordinates $1:(0,2\varphi)$, $2:(\pi/2-\varphi,\pi/2+\varphi)$, $3:(\pi-2\varphi,\pi)$, $4:(2\varphi-\pi,\pi)$, where $\varphi=\arccos(1/3)$. The coordinates of the other green points follow by symmetry.

Note that $|\mathcal{AB}|=|\mathcal{A}|\,|\mathcal{B}|$ and $(\mathcal{AB})^*=\mathcal{B}^*\mathcal{A}^*$. A *unit* quaternion $\mathcal{U}$ with $|\mathcal{U}|=1$ can be written as $\left(\cos\frac{1}{2}\psi,\sin\frac{1}{2}\psi\,\boldsymbol{u}\right)$ for some angle ψ and unit vector $\boldsymbol{u}$, and for any vector $\boldsymbol{f}$ the transformation $\boldsymbol{f}\mapsto\mathcal{U}\boldsymbol{f}\mathcal{U}^*$ yields a rotation of $\boldsymbol{f}$ by angle ψ about an axis in the direction specified by $\boldsymbol{u}$.

In the quaternion model, the hodograph of a quintic spatial PH curve is generated from a quadratic quaternion polynomial

$$\mathcal{A}(\xi)=\mathcal{A}_0(1-\xi)^2+\mathcal{A}_1 2(1-\xi)\xi+\mathcal{A}_2\xi^2 \tag{22}$$

with coefficients $\mathcal{A}_r=u_r+v_r\mathbf{i}+p_r\mathbf{j}+q_r\mathbf{k}$, $r=0,1,2$ through the product

$$\boldsymbol{r}'(\xi)=\mathcal{A}(\xi)\mathbf{i}\mathcal{A}(\xi)^*. \tag{23}$$

We assume canonical Hermite data, with $\boldsymbol{r}(0)=(0,0,0)$ and $\boldsymbol{r}(1)=(1,0,0)$ and end derivatives $\boldsymbol{d}_0,\boldsymbol{d}_1$. Matching the derivatives yields the equations

$$\mathcal{A}_0\mathbf{i}\mathcal{A}_0^*=\boldsymbol{d}_0 \qquad \text{and} \qquad \mathcal{A}_2\mathbf{i}\mathcal{A}_2^*=\boldsymbol{d}_1 \tag{24}$$

for $\mathcal{A}_0$ and $\mathcal{A}_2$. With $\exp(\phi\mathbf{i}):=(\cos\phi,\sin\phi\,\mathbf{i})$, the solutions [8] are

$$\mathcal{A}_0=\sqrt{d_0}\boldsymbol{n}_0\exp(\phi_0\mathbf{i}), \qquad \mathcal{A}_2=\sqrt{d_1}\boldsymbol{n}_1\exp(\phi_2\mathbf{i}), \tag{25}$$

where ϕ_0, ϕ_2 are free parameters, $d_0=|\boldsymbol{d}_0|$, $d_1=|\boldsymbol{d}_1|$, $\boldsymbol{\delta}_0=\boldsymbol{d}_0/d_0$, $\boldsymbol{\delta}_1=\boldsymbol{d}_1/d_1$, and $\boldsymbol{n}_0$, $\boldsymbol{n}_1$ are the unit bisectors of $\mathbf{i}$ and $\boldsymbol{\delta}_0$, $\boldsymbol{\delta}_1$. Moreover, the end point interpolation condition yields [8] the equation

$$(3\mathcal{A}_0+4\mathcal{A}_1+3\mathcal{A}_2)\mathbf{i}(3\mathcal{A}_0+4\mathcal{A}_1+3\mathcal{A}_2)^*=\boldsymbol{d}, \tag{26}$$

where

$$\boldsymbol{d}=120\mathbf{i}-15(\boldsymbol{d}_0+\boldsymbol{d}_1)+5(\mathcal{A}_0\mathbf{i}\mathcal{A}_2^*+\mathcal{A}_2\mathbf{i}\mathcal{A}_0^*). \tag{27}$$

With $d=|\boldsymbol{d}|$ and $\boldsymbol{\delta}=\boldsymbol{d}/d$, Equation (26) has solutions of the form

$$\mathcal{A}_1=\frac{\sqrt{d}\,\boldsymbol{n}\exp(\phi_1\mathbf{i})-3(\mathcal{A}_0+\mathcal{A}_2)}{4}, \qquad \boldsymbol{n}=\frac{\mathbf{i}+\boldsymbol{\delta}}{|\mathbf{i}+\boldsymbol{\delta}|}. \tag{28}$$

Since the interpolants depend only on the *differences* of the angular variables ϕ_0, ϕ_1, ϕ_2 we may henceforth set $\phi_1=0$ without loss of generality [6]. Thus, in general, there is a two-parameter family of spatial PH quintic interpolants.

3.1 The case $\phi_2 - \phi_0 =$ constant

A one-dimensional specialization of the two-dimensional space of spatial PH quintic Hermite interpolants arises from the imposition of a relation between ϕ_0 and ϕ_2. We consider now the simplest case, $\phi_2 - \phi_0 =$ constant.

Proposition 8. *The condition $\phi_2 - \phi_0 = \delta\phi$ identifies, for each fixed $\delta\phi$, a one-parameter family of spatial PH quintic interpolants to given first-order Hermite data that have identical arc lengths.*

Proof. The total arc length of a spatial PH quintic Hermite interpolant can be expressed [4, Lemma 28.1] as

$$S = \frac{1}{120}\big(|3\mathcal{A}_0 + 4\mathcal{A}_1 + 3\mathcal{A}_2|^2 + 15(d_0 + d_1) - 5(\mathcal{A}_0\mathcal{A}_2^* + \mathcal{A}_2\mathcal{A}_0^*)\big).$$

From (26) and (27), we can replace $|3\mathcal{A}_0 + 4\mathcal{A}_1 + 3\mathcal{A}_2|^2$ by $|120\,\mathbf{i} - 15(\boldsymbol{d}_0 + \boldsymbol{d}_1) + 5(\mathcal{A}_0\,\mathbf{i}\,\mathcal{A}_2^* + \mathcal{A}_2\,\mathbf{i}\,\mathcal{A}_0^*)|$, and on using (25) we obtain

$$\begin{aligned}
\mathcal{A}_0\mathcal{A}_2^* + \mathcal{A}_2\mathcal{A}_0^* &= 2\sqrt{d_0 d_1}\big(\cos\delta\phi\ \boldsymbol{n}_0\cdot\boldsymbol{n}_1 + \sin\delta\phi\ \mathbf{i}\cdot(\boldsymbol{n}_0\times\boldsymbol{n}_1)\big),\\
\mathcal{A}_0\,\mathbf{i}\,\mathcal{A}_2^* + \mathcal{A}_2\,\mathbf{i}\,\mathcal{A}_0^* &= 2\sqrt{d_0 d_1}\big(\cos\delta\phi\big[(\mathbf{i}\cdot\boldsymbol{n}_0)\,\boldsymbol{n}_1 + (\mathbf{i}\cdot\boldsymbol{n}_1)\,\boldsymbol{n}_0 - (\boldsymbol{n}_0\cdot\boldsymbol{n}_1)\mathbf{i}\big] - \sin\delta\phi\ \boldsymbol{n}_0\times\boldsymbol{n}_1\big).
\end{aligned}$$

Thus, the total arc length depends only on the *difference* $\delta\phi = \phi_2 - \phi_0$. □

The dependence of S on $\delta\phi$ has a single minimum and maximum [8], which identify *helical curves* characterized [16] by a constant curvature/torsion ratio and a unit tangent $\boldsymbol{t}$ that makes a fixed angle ψ (the helix angle) with a fixed unit vector $\boldsymbol{a}$ (the helix axis) — that is, $\boldsymbol{a}\cdot\boldsymbol{t} = \cos\psi$. This condition implies [10] that any helical curve with a *polynomial* parameterization is a PH curve.

3.2 Specialization to the planar case

Equations (24) and (26) are the spatial analogs of Equations (2) and (4) for the planar case. For spatial PH curves, the condition for any given canonical-form data (with $\boldsymbol{p}_1 - \boldsymbol{p}_0 = \mathbf{i}$) to be consistent with a planar curve is

$$\mathbf{i}\cdot(\boldsymbol{d}_0\times\boldsymbol{d}_1) = 0. \tag{29}$$

When this is satisfied, a planar solution will reside in the plane through the x-axis containing the derivative vectors $\boldsymbol{d}_0$ and $\boldsymbol{d}_1$. Let $\vartheta_0, \vartheta_1 \in [0,\pi]$ and $\psi_0, \psi_1 \in [0, 2\pi)$ be the polar and azimuthal angles of $\boldsymbol{d}_0$ and $\boldsymbol{d}_1$ relative to the x-axis. Then ψ_0, ψ_1 may differ only by an integer multiple of π, and if ψ is either of these angles, the unit quaternion $\mathcal{U} = \cos\frac{1}{2}\psi - \sin\frac{1}{2}\psi\,\mathbf{i}$ defines a rotation through angle $-\psi$ about $\mathbf{i}$ through the mappings

$$\boldsymbol{d}_0 \mapsto \mathcal{U}\,\boldsymbol{d}_0\,\mathcal{U}^*, \qquad \boldsymbol{d}_1 \mapsto \mathcal{U}\,\boldsymbol{d}_1\,\mathcal{U}^*, \tag{30}$$

so the transformed derivatives lie in the (x,y)-plane. Thus we may henceforth assume, without loss of generality, that $\boldsymbol{d}_0$, $\boldsymbol{d}_1$ have no z component.

Remark 4. Since (23) generates a pure vector, the basis for the Euclidean plane in the spatial model is $(\mathbf{i},\mathbf{j})$ rather than $(1,\mathrm{i})$ in the planar model. Thus, to establish a correspondence between these models, we must identify $\mathbf{i}$ and $\mathbf{j}$ components in the former with the 1 and i components in the latter.

Proposition 9. *If the Hermite data satisfies the planarity condition in (29) and the transformation in (30) is applied, the spatial Hermite interpolation problem specified by the quaternion equations (24) and (26) specializes to the planar Hermite interpolation specified by the complex equations (2) and (4) when the angular parameters ϕ_0 and ϕ_2 in (25) are both integer multiples of π.*

Proof. Setting $\boldsymbol{d}_0 = d_0(\lambda_0\mathbf{i} + \mu_0\mathbf{j})$, $\boldsymbol{d}_1 = d_1(\lambda_1\mathbf{i} + \mu_1\mathbf{j})$ and $\phi_0 = m\pi$, $\phi_2 = n\pi$ for integers m and n we have $\mathcal{A}_0 = s_0\sqrt{d_0}\boldsymbol{n}_0$, $\mathcal{A}_2 = s_1\sqrt{d_1}\boldsymbol{n}_1$ from (25), where

$$\boldsymbol{n}_0 = \frac{(1+\lambda_0)\mathbf{i} + \mu_0\mathbf{j}}{\sqrt{2(1+\lambda_0)}}, \qquad \boldsymbol{n}_1 = \frac{(1+\lambda_1)\mathbf{i} + \mu_1\mathbf{j}}{\sqrt{2(1+\lambda_1)}},$$

and $s_0 = \pm 1$ and $s_1 = \pm 1$ for m and n even or odd. On identifying $(\mathbf{i},\mathbf{j})$ with $(1,\mathrm{i})$ these expressions for $\mathcal{A}_0$, $\mathcal{A}_2$ agree with the formulae in (3) for $\boldsymbol{w}_0$, $\boldsymbol{w}_2$ with $(\cos\theta_0, \sin\theta_0) = (\lambda_0, \mu_0)$ and $(\cos\theta_1, \sin\theta_1) = (\lambda_1, \mu_1)$.

Now with $\boldsymbol{w}_0^2 = \boldsymbol{d}_0$ and $\boldsymbol{w}_2^2 = \boldsymbol{d}_1$, Equation (4) can be formulated in a manner analogous to Equations (26) and (27) as

$$(3\boldsymbol{w}_0 + 4\boldsymbol{w}_1 + 3\boldsymbol{w}_2)^2 = \boldsymbol{d}, \qquad \boldsymbol{d} = 120 - 15(\boldsymbol{d}_0 + \boldsymbol{d}_1) + 10\boldsymbol{w}_0\boldsymbol{w}_2. \tag{31}$$

The 1, i components of the expression for $10\boldsymbol{w}_0\boldsymbol{w}_2$ in (31) evaluate to

$$5s_0s_1\sqrt{d_0d_1}\frac{(1+\lambda_0)(1+\lambda_1)-\mu_0\mu_1}{\sqrt{(1+\lambda_0)(1+\lambda_1)}}, \qquad 5s_0s_1\sqrt{d_0d_1}\frac{(1+\lambda_0)\mu_1+\mu_0(1+\lambda_1)}{\sqrt{(1+\lambda_0)(1+\lambda_1)}},$$

and evaluating the term $5(\mathcal{A}_0\,\mathbf{i}\,\mathcal{A}_2^* + \mathcal{A}_2\,\mathbf{i}\,\mathcal{A}_0^*)$ in (27) gives exactly the same expressions for its $\mathbf{i}$, $\mathbf{j}$ components, so the vectors $\boldsymbol{d}$ in (27) and (31) agree.

Having established the correspondence of $\mathcal{A}_0, \mathcal{A}_2, \boldsymbol{d}$ and $\boldsymbol{w}_0, \boldsymbol{w}_2, \boldsymbol{d}$ in the spatial and planar cases, we now consider

$$\mathcal{A}_1 = \frac{\sqrt{d}\,\boldsymbol{n} - 3(\mathcal{A}_0 + \mathcal{A}_2)}{4} \qquad \text{and} \qquad \boldsymbol{w}_1 = \frac{\sqrt{\boldsymbol{d}} - 3(\boldsymbol{w}_0 + \boldsymbol{w}_2)}{4}.$$

As before, we use $\phi_1 = 0$ in $\mathcal{A}_1$ and a unique complex root of $\boldsymbol{d}$ in $\boldsymbol{w}_1$. We need only consider $\sqrt{d}\,\boldsymbol{n}$ and $\sqrt{\boldsymbol{d}}$ in the above expressions. With $\boldsymbol{d} = d(\lambda\,\mathbf{i} + \mu\,\mathbf{j})$ and $\boldsymbol{d} = d(\lambda + \mu\,\mathrm{i})$ in the former and latter cases, we obtain the equivalence

$$\mathcal{A}_1 = \sqrt{d}\frac{(1+\lambda)\mathbf{i} + \mu\,\mathbf{j}}{\sqrt{2(1+\lambda)}} \qquad \text{and} \qquad \boldsymbol{w}_1 = \sqrt{d}\frac{(1+\lambda) + \mu\,\mathrm{i}}{\sqrt{2(1+\lambda)}}.$$

□

By Proposition 9, all the degenerate cases in the planar problem described in Section 2 are subsumed as special cases of the spatial Hermite interpolation problem when ϕ_0 and ϕ_2 are integer multiples of π. Otherwise, the solutions of spatial Hermite interpolation problem are, in general, non-planar curves — even when the planarity condition in (29) is satisfied.

4 Closure

Because of their non-linear nature, Pythagorean-hodograph (PH) curves are not amenable to characterization or construction based on standard control-polygon schemes — except [12] in the elementary case of planar PH cubics. Consequently, the interpolation of discrete data (end points and derivatives) is the standard approach to constructing PH curves. This entails the solution of systems of quadratic equations, expressed in terms of the complex number and quaternion algebras for planar and spatial PH curves, and a multiplicity of formal solutions that match prescribed Hermite data.

The present study identifies and characterizes singular instances of these Hermite interpolation problems, which incur reductions in the cardinality of the solution space. For the planar PH quintics, certain configurations of the end derivatives result in the degeneration of the generic four distinct Hermite interpolants to just three (two "simple" and one "double") distinct solutions. The computed examples suggest that the "double" solution is never the good interpolant (free of tight loops), and it would be of interest to see if this can be rigorously verified. For the spatial PH quintics, the Hermite interpolation problem generally yields a two-parameter family of solutions, and enforcing a fixed difference between the parameters generates a one-parameter family of distinct space curves with identical arc lengths. Finally, for Hermite data compatible with a planar curve, certain fixed values of the two parameters in the spatial PH curve solution establish a formal correspondence between the planar and spatial Hermite interpolants, indicating that the degenerate instances of the former are subsumed by the latter.

Acknowledgement

The third author would like to thank the Faculty of Informatics of the Università della Svizzera italiana (USI) for granting him a Masters Research Scholarship (MaRS), during which this research was conducted.

References

[1] H. I. Choi, R. T. Farouki, S.-H. Kwon, and H. P. Moon. Topological criterion for selection of quintic Pythagorean-hodograph Hermite interpolants. *Computer Aided Geometric Design*, 25(6):411–433, Aug. 2008.

[2] H. I. Choi, D. S. Lee, and H. P. Moon. Clifford algebra, spin representation, and rational parameterization of curves and surfaces. *Advances in Computational Mathematics*, 17(1–2):5–48, July 2002.

[3] R. T. Farouki. The conformal map $z \to z^2$ of the hodograph plane. *Computer Aided Geometric Design*, 11(4):363–390, Aug. 1994.

[4] R. T. Farouki. *Pythagorean-Hodograph Curves: Algebra and Geometry Inseparable*, volume 1 of *Geometry and Computing*. Springer, Berlin, 2008. ISBN 978-3-540-73398-0.

[5] R. T. Farouki. Construction of G^1 planar Hermite interpolants with prescribed arc lengths. *Computer Aided Geometric Design*, 46:64–75, Aug. 2016.

[6] R. T. Farouki, M. al-Kandari, and T. Sakkalis. Hermite interpolation by rotation-invariant spatial Pythagorean-hodograph curves. *Advances in Computational Mathematics*, 17(4):369–383, Nov. 2002.

[7] R. T. Farouki, M. al-Kandari, and T. Sakkalis. Structural invariance of spatial Pythagorean hodographs. *Computer Aided Geometric Design*, 19(6):395–407, June 2002.

[8] R. T. Farouki, C. Giannelli, C. Manni, and A. Sestini. Identification of spatial PH quintic Hermite interpolants with near optimal shape measures. *Computer Aided Geometric Design*, 25(4–5):274–297, May–June 2008.

[9] R. T. Farouki, C. Giannelli, and A. Sestini. New developments in theory, algorithms, and applications for Pythagorean-hodograph curves. In C. Giannelli and H. Speelers, editors, *Advanced Methods for Geometric Modeling and Numerical Simulation*, volume 35 of *Springer INdAM Series*, pages 127–177. Springer, Cham, 2019.

[10] R. T. Farouki, C. Y. Han, C. Manni, and A. Sestini. Characterization and construction of helical polynomial space curves. *Journal of Computational and Applied Mathematics*, 162(2):365–392, Jan. 2004.

[11] R. T. Farouki and C. A. Neff. Hermite interpolation by Pythagorean-hodograph quintics. *Mathematics of Computation*, 64(212):1589–1609, Oct. 1995.

[12] R. T. Farouki and T. Sakkalis. Pythagorean hodographs. *IBM Journal of Research and Development*, 34(5):736–752, Sept. 1990.

[13] R. T. Farouki and Z. Šír. Rational Pythagorean-hodograph space curves. *Computer Aided Geometric Design*, 28(2):75–88, Feb. 2011.

[14] C. Y. Han, H. P. Moon, and S.-H. Kwon. A new selection scheme for spatial Pythagorean hodograph quintic Hermite interpolants. *Computer Aided Geometric Design*, 78:Article 101827, 18 pages, Mar. 2020.

[15] S. H. Kim and H. P. Moon. Rectifying control polygon for planar Pythagorean hodograph curves. *Computer Aided Geometric Design*, 54:1–14, May 2017.

[16] E. Kreyszig. *Differential Geometry*, volume 11 of *Mathematical Expositions*. University of Toronto Press, Toronto, 1959. ISBN 978-1-4875-8945-5.

[17] H. P. Moon, R. T. Farouki, and H. I. Choi. Construction and shape analysis of PH quintic Hermite interpolants. *Computer Aided Geometric Design*, 18(2):93–115, Mar. 2001.

[18] H. Pottmann. Rational curves and surfaces with rational offsets. *Computer Aided Geometric Design*, 12(2):175–192, Mar. 1995.

[19] L. Romani and F. Montagner. Algebraic-trigonometric Pythagorean-hodograph space curves. *Advances in Computational Mathematics*, 45(1):75–98, Feb. 2019.

[20] L. Romani, L. Saini, and G. Albrecht. Algebraic-trigonometric Pythagorean-hodograph curves and their use for Hermite interpolation. *Advances in Computational Mathematics*, 40(5–6):977–1010, Dec. 2014.